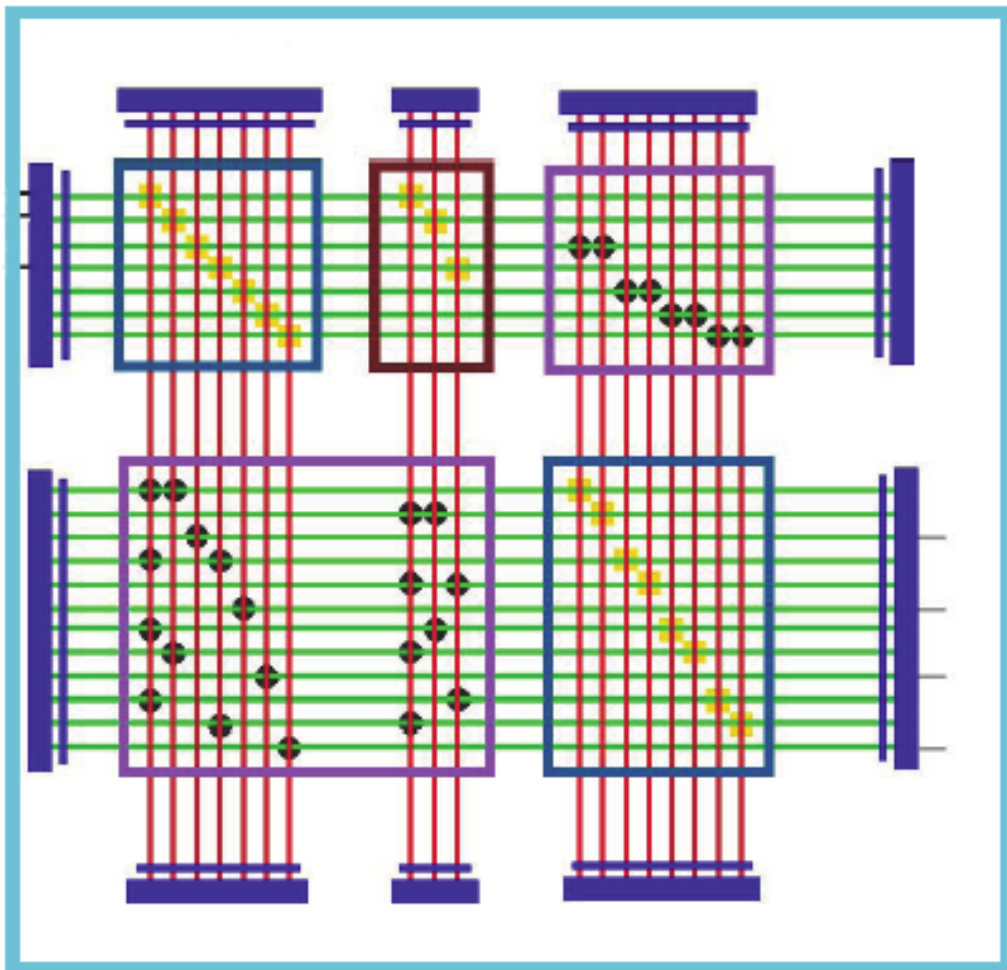

Designing a Nanoelectronic Circuit to Control a Millimeter-scale Walking Robot

Alexander J. Gates

November 2004

MP 04W0000312

MITRE
McLean, Virginia



Designing a Nanoelectronic Circuit to Control a Millimeter-scale Walking Robot

Alexander J. Gates

November 2004

MITRE Nanosystems Group

MP 04W0000312

e-mail: nanotech@mitre.org
WWW: <http://www.mitre.org/tech/nanotech>

Sponsor MITRE MSR Program
Project No. 51MSR89G
Dept. W809

Approved for public release;
distribution unlimited.

Copyright © 2004 by The MITRE Corporation.
All rights reserved.

Abstract

A novel nanoelectronic digital logic circuit was designed to control a millimeter-scale walking robot using a nanowire circuit architecture. This nanoelectronic circuit has a number of benefits, including extremely small size and relatively low power consumption. These make it ideal for controlling microelectromechanical systems (MEMS), such as a millirobot. Simulations were performed using a SPICE circuit simulator, and unique device models were constructed in this research to assess the function and integrity of the nanoelectronic circuit's output. It was determined that the output signals predicted for the nanocircuit by these simulations meet the requirements of the design, although there was a minor signal stability issue. A proposal is made to ameliorate this potential problem. Based on this proposal and the results of the simulations, the nanoelectronic circuit designed in this research could be used to begin to address the broader issue of further miniaturizing circuit-micromachine systems.

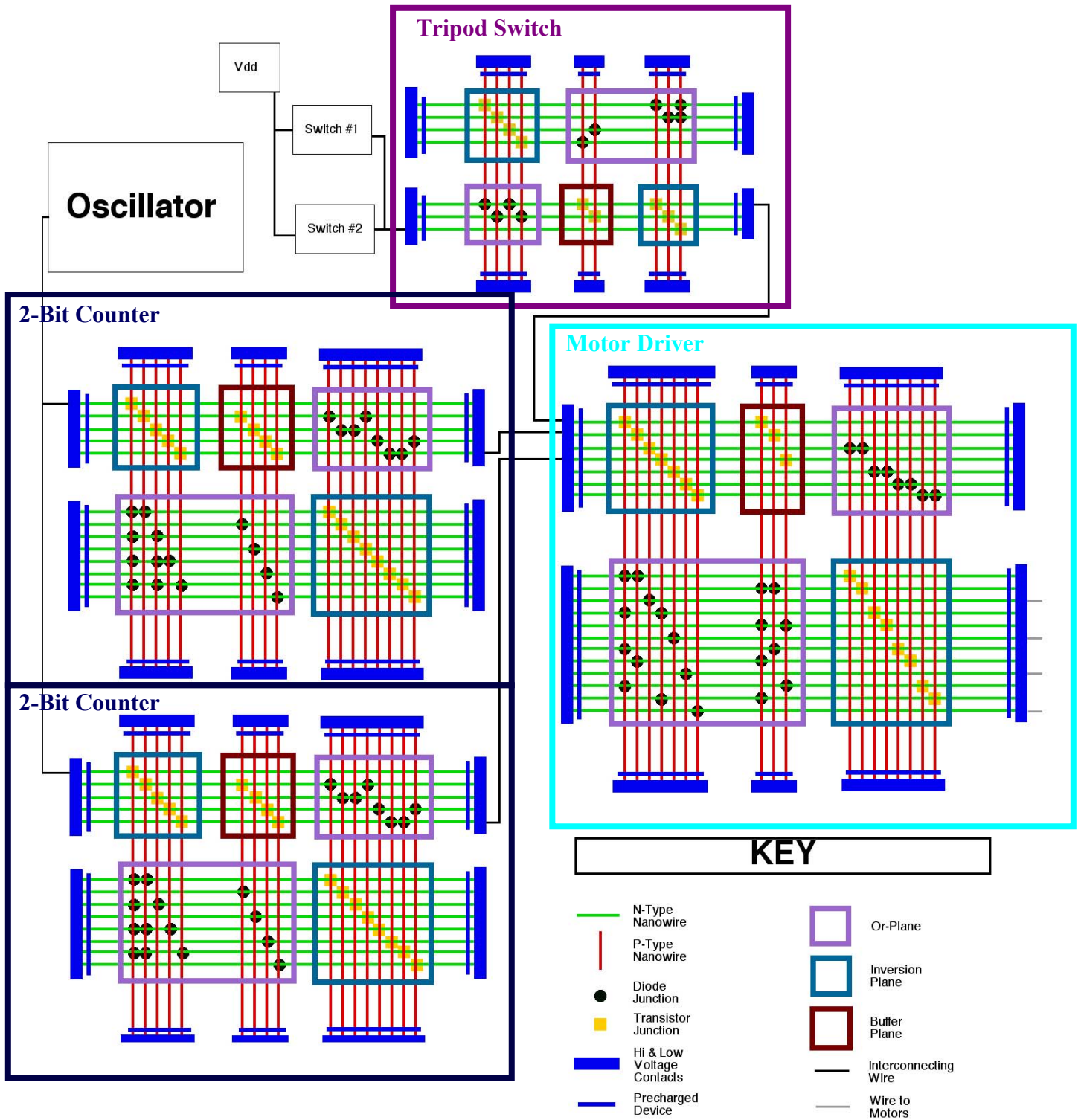
I. Introduction

The purpose of this paper is to describe the novel nanoelectronic digital logic circuit shown in Figure 1, which has been designed by this author to control a millimeter-scale walking robot. An example of such a millimeter-scale robot is depicted in Figure 2.

There are a number of challenges in the design of novel nanoelectronic circuits [1-4]. However, they have the potential to build computers and device controllers that are much denser and therefore much smaller than those presently using conventional microelectronics [2]. In addition, nanoelectronics hold the promise of using much less power than conventional microelectronics, allowing systems that use such computers to be made much smaller [2]. Thus, it is the goal of this research to utilize nanoelectronic circuits, such as the one in Figure 1, to address the broader issue of further miniaturizing circuit-micromachine systems.

As an initial effort towards this goal, this investigation proceeded in several steps to design a nanoelectronic circuit to control the mechanism for a millimeter-scale walking robot. In the first step, the millirobot control circuit was laid out in a functional schematic. Second, it was mapped (transferred) to a Nanowire-based Dynamic Programmable Logic Array circuit architecture developed by DeHon of Caltech [5-7]. This circuit architecture was chosen due to the exciting development of the architecture's nanowire-based nanoelectronic components by Charles Lieber of Harvard University [8-11], which suggests that such nanowire-based nanocomputer circuits might be built in the near future. Third, the performance of the circuit structure implementing the nanowire circuit components was simulated using a SPICE circuit simulator [12]. The circuit simulation incorporated device models that were constructed using several approximations for the capacitances and resistances of the nanoelectronic components. Circuit descriptions were written for the inverter and buffer sub-circuits. Finally, simulations to test the functionality of the circuit designs were conducted. These employed input signals that emulate those likely to be used in a millimeter-scale walking robot.

Figure 1. The layout of the entire nanowire based nanoelectronic controller to produce a millirobot's tripod gait, as designed by the author.



The results of these simulations are presented below in Section IV.B. Upon analysis, the results of these simulations revealed that the nanoelectronic circuit did generate signals with the desired shape and spacing. Still, the signal stability was not immediately sufficient to ensure reliable control of a millirobot. The author has proposed a solution to address this problem. On that basis, the nanoelectronic control circuit designed here should be able to coordinate the legs and their corresponding actuators on a millirobot. It should also deliver the benefits of a very small, low power electronic system where it is much needed on a tiny machine.

II. Background

A. Millimeter-Scale Walking Robot

An understanding of the major elements of the design for the next-generation millirobot helps to explain the structure and function of the millirobot control circuit. Presently, there are several different designs for millimeter-scale walking robots, including a version that has already been constructed by researchers at the University of California at Berkeley [13-16]. All of these designs have utilized off-robot power sources and control circuits, or they have dragged these necessary components awkwardly behind the main body, greatly decreasing the mobility and efficiency of the tiny robot. However, researchers at the MITRE Corporation are designing a millirobot that will utilize self-contained power and control systems [17].

The MITRE millimeter-scale walking robot, an example of the target systems for the author's control circuit, was designed to be fabricated on a silicon wafer. This imposes a planar construction requirement where three-dimensional structures must fold into a shape. As depicted in Figure 2, there will be six legs, each of which will have two degrees of freedom. Following the millirobot mechanism designers at the MITRE Corporation [17], it is assumed here that the millirobot will walk using the tripod gait employed by insects [18,19] which are the same size as that projected for the millirobot.

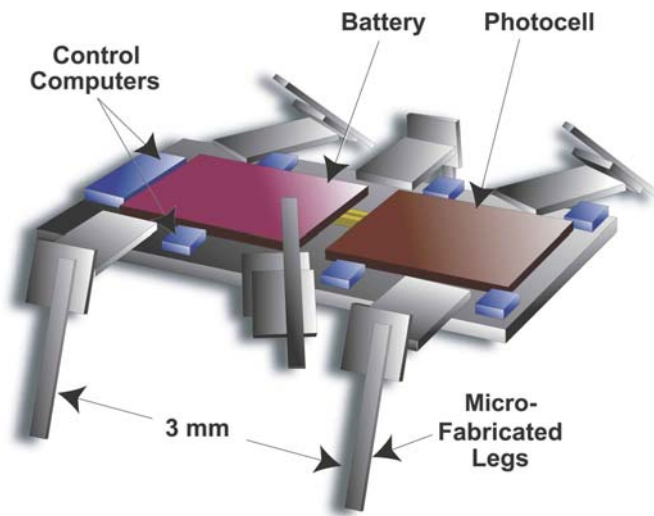


Figure 2. Design for a millirobot as originally designed by Routenberg and Ellenbogen at the MITRE Corporation [17]. The present author's original control circuit is designed to coordinate the leg movements on tiny robots such as this insect-like walking robot.

The tripod gait requires the 6 legs of the robot to be split into two groups or tripods. Each tripod includes the two end legs on one side and the center leg on the opposite side, as represented in Figure 3. To walk forward, one tripod lifts its legs and moves them forward while the other tripod pushes backwards until its legs return to their rearmost position. It is this motion of the twin tripods that must be generated and modulated by the nanoelectronic control circuit designed in the research described here.

To produce this well coordinated leg motion, the nanoelectronic circuits will have to control the tiny drive mechanism formed by the multiple comb drives that the millirobot designers plan to use to supply mechanical power for the legs [17]. Comb drives, as depicted in Figure 4(A), are well known microelectromechanical systems (MEMS) [20-24]. The drives are shaped like two interlocking combs, one of which is fastened to the underlying substrate while the other is attached to a spring and the output track. In most such electrostatic drives, the teeth of the combs are pulled together by a pulsed voltage of approximately 50V. The teeth are then restored to their original positions by the spring when the voltage is dropped to around 0V [23,24]. The resonating motion produced can be transferred to linear motion by combining a series of comb drives with a shuttle, gear, or clutch type drive train as depicted by Figure 4(B), all of which have been constructed in many micrometer-scale MEMS systems, including millirobot prototypes built at MITRE [17].

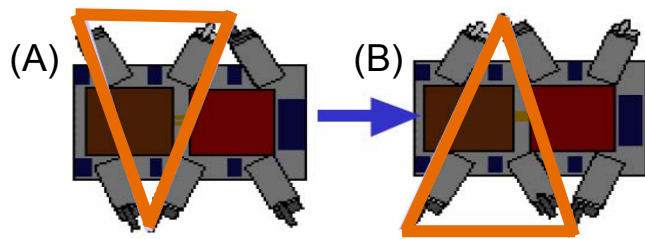


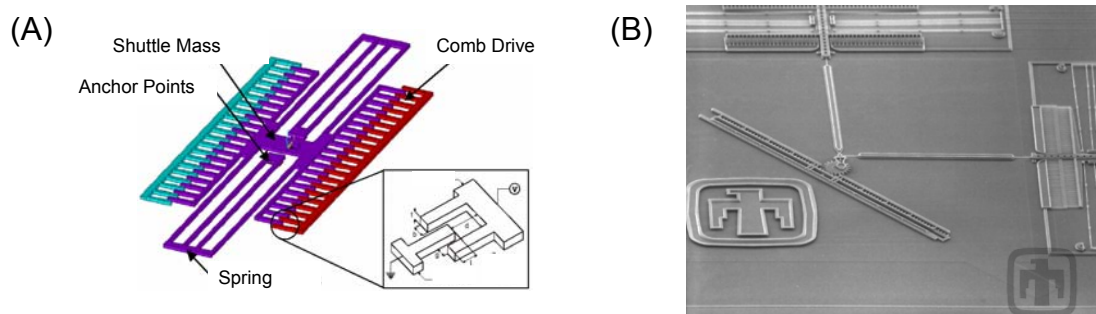
Figure 3. The operation of the millirobot leg segregates them into the 2 “tripods”. The forward and reverse motion of the legs is also depicted as the millirobot takes half a step from (A) to (B).

Because a millirobot can only carry very small power sources, all its electrical subsystems must consume very low power to minimize energy drain and maximize operational life. This presents an additional challenge for the job of designing the millirobot control circuits, which is addressed below in detail.

B. Nanometer-Scale Computational Systems

The nanoelectronic circuit designed in this research adapts and applies recent innovations in nanoelectronics technology. Several different nanometer-scale structures currently are being investigated as possible replacements for the bulk silicon metal-oxide semiconductor field effect transistor (MOSFET) that is the basis for conventional microprocessor technology. Of these, silicon and germanium nanowires are seen by the author as being most viable for actually implementing the nanoelectronic control circuit designed here. Such semiconductor nanowires are single-crystal filaments that range in diameter from two to one hundred nanometers, and they can reach thirty micrometers in length [26]. They are grown easily with predictable control over

Figure 4. (A) Typical MEMS comb drive as depicted in [24]. (B) Two such comb drives can be linked together and attached to a linear track as fabricated at Los Alamos National Laboratories [25] and utilized in the millirobot design shown in Figure 2. The purpose of the nanoelectronic circuitry designed in this paper is to control the motion in the drive assemblies.

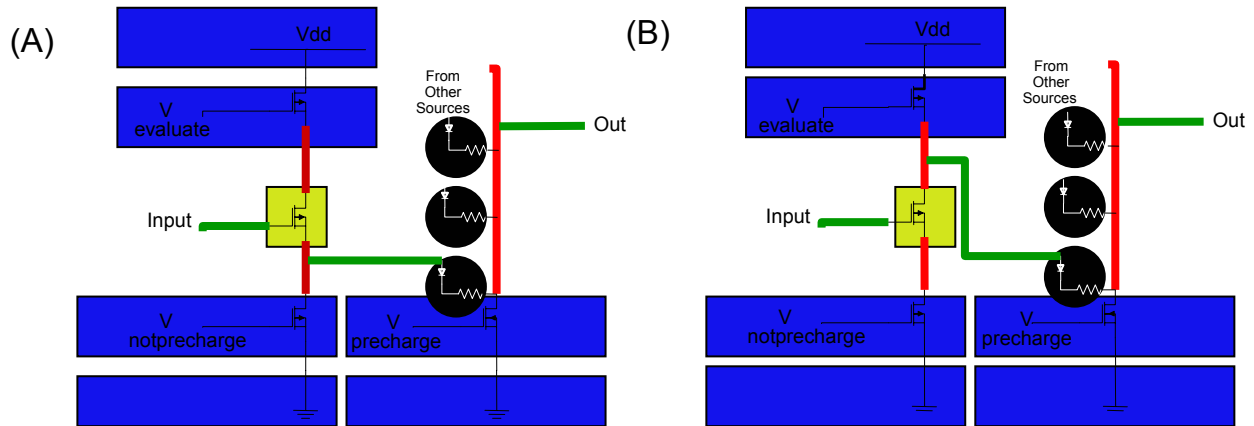


diameter size and doping properties [27]. Through a flow deposition process, nanowires can be manipulated directionally and positioned to form a layer of parallel wires orientated on a substrate [27]. Arranged in crossed pairs, such nanowires can be made to form a transistor at their junction. These nanowire nanotransistors provide the same function as the current bulk silicon microelectronic MOSFET, except up to one hundred times smaller [28]. Large numbers of nanowires arranged in crossed arrays have already been used to form memory cells as well as logic arrays [29,30].

The author also identified the Nanowire-based Dynamic Programmable Logic Array architecture proposed at Caltech by Andre DeHon as the most promising nanowire circuit architecture [5,6]. This nanoprocessor architecture has been adapted by the author for the purpose of millirobot control. One of the advantages of using DeHon's nanowire architecture for this purpose is that it is a Programmable Logic Array (PLA). This means that chips could be mass produced containing flexible, generic layouts of the architecture framework and later programmed by the end user to perform any of a range of specific functions. No physical fabrication processes are needed to specialize the chip's function.

DeHon's circuit architecture utilizes nanowire transistors and diodes to perform three basic logic functions: inversion, buffering, and OR logic [5]. The nanowire transistors are to be formed at the cross points of heavily doped regions of n-type and p-type nanowires [5]. (Such n-type materials are doped with a permanent excess of electrons, while p-type materials are doped with a permanent electron deficiency in the bonds of the atoms that form the material.) Within the nanowire grid, the n-type wires will act as the gate while the p-type nanowires form the source and drain. Both the inverter and buffer consist of four transistors, three p-type and one n-type, as shown in Figure 5(A) and 5(B).

Figure 5. Element (A) is a design for an inverter circuit while (B) represents the buffer. The conventional representations for the circuit components are overlaid above their corresponding representations in the nanometer-scale design for the millirobot control circuit. (Based on buffer and inverter designs in Ref. [5].)



According to DeHon’s architecture, the two transistors on the bottom of the inverter displayed in Figure 5(A) are known as the precharge transistors. The p-type precharge transistor receives a signal from the “notprecharge” clock (the inverse of the precharge clock) that turns the transistor on and connects the line under the drain of the input transistor to ground. The n-type transistor receives a signal from the precharge clock that turns it on and also connects the output line down to ground. The evaluate transistor, located on the top of the inverter, is then turned on by the evaluate clock. Once it is switched on, the inverse voltage of whichever signal is entering through the input line is connected to the output. Therefore, any signal processed by an inverter junction enters through the n-type wire and exits through the p-type wire. The buffer, shown in Figure 5(B), operates in much the same way except that the output line is located above the input transistor, taking on the same properties as the input. Again, any signal that is processed by a buffer junction enters through the n-type wire and exits through the p-type wire [5].

OR logic is implemented through the usage of programmable diode junctions [5]. Much like the nanowire junction transistor, the nanowire diode junction is formed at the junction of n-type and p-type nanowires. Within this architecture, the anode of the diode is the p-type

nanowire and the cathode is the n-type nanowire. As a result, any voltage change in the p-type nanowire will be transferred to the n-type nanowire. However, any voltage change in the n-type nanowire will not affect the p-type nanowire [5]. This is because the p-type nanowires have low electron concentrations and are unaffected by any decrease in electron concentration of the n-type nanowire. Several diode junctions can be formed on one n-type nanowire resulting in an OR gate.

III. Methods

As previously described, there were four major steps in the design of the nanoelectronic circuit to control the MEMS electrostatic actuators on a millimeter-scale walking robot. This section describes these steps in detail. The first step was to construct the block level diagram for the controller, which is shown superimposed over Figure 6. This was accomplished by analyzing the purpose of the circuit, then identifying components used in conventional digital logic circuit design that would achieve this goal with only minor adjustments.

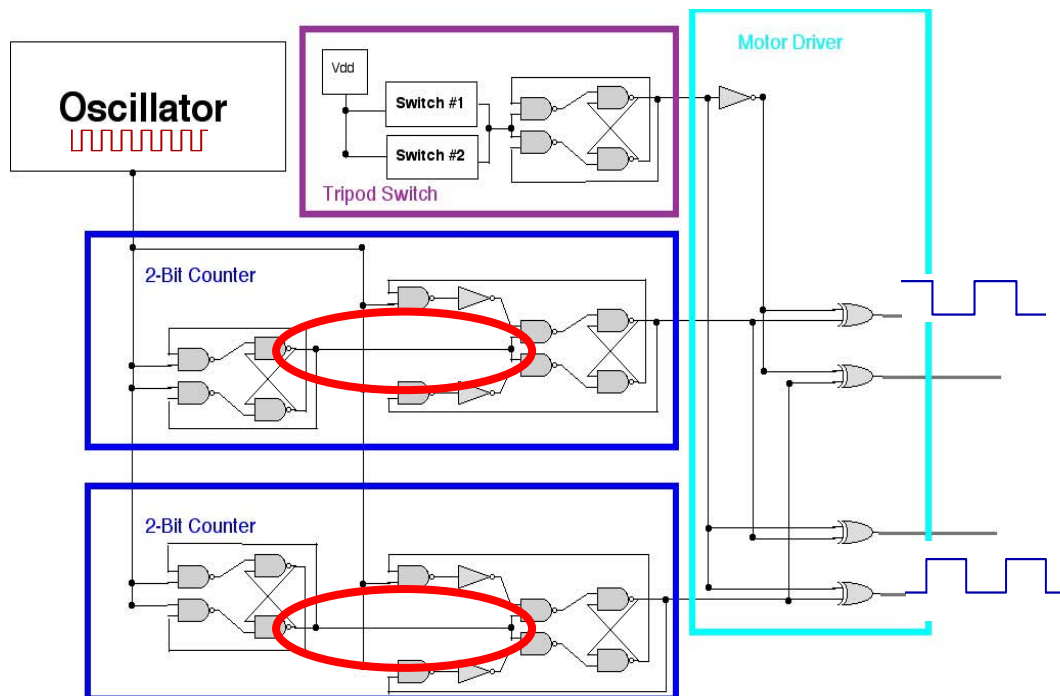


Figure 6. The logic-based control circuit for a tripod gait in a millimeter-scale walking robot. Under the oscillator there is an emulated oscillator signal while at two of the output lines from the motor driver there are the logically simulated outputs. The two red ovals denote the different use of clocking in the dual 2-bit counters.

The second step was to design a logic level circuit diagram, depicted within the blocks in Figure 6. There were no limitations on which logic elements could be utilized, although it was found that only the NAND, XOR, and inverter logic gates were needed. To perfect and test for errors in the logic-level design, the logic circuit was simulated using the LogicSim 3.0b logic simulation software [31]. Calculations also were performed for specific elements using algebraic logic equations and logic tables.

The third step was to produce a circuit structure diagram by mapping the conventional logic circuit into the DeHon nanowire circuit architecture. The final nanowire-based circuit structure is displayed in Figure 1. Mapping the logic-level design to this circuit structure required that the logic circuit be expressed in terms of OR and inverter logic components rather than in terms of the NAND and XOR logic originally utilized in the design of the logic circuit shown in Figure 6. Therefore, this logic circuit was redesigned using De Morgan's Theorem from Boolean algebra. Component alterations were double-checked using techniques similar to those previously mentioned in the design of the original logic circuit. Once the logic circuit was correctly redesigned, it was transferred to the DeHon nanowire architecture. Signal paths were laid out with an offset rectangular spiral, shown in Figure 7, as opposed to a randomized fabrication representation.

The fourth step was to assess components of the nanowire circuit using the SPICE circuit

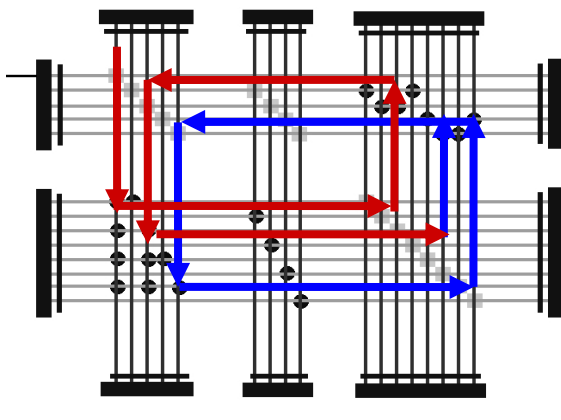


Figure 7. The offset rectangular spiral device layout is depicted by the red arrows. All nanoelectronic circuits designed by this research utilize this device layout. Additionally, as depicted by the blue arrows, the nanowire architecture easily accommodated looping in circuit designs.

simulator. Because there is still only limited experimental data available concerning the behavior of the nanowire-based devices, device models were constructed utilizing several approximations for capacitances and resistances [1]. The most notable of these approximations modeled the gate oxide as being several orders of magnitude thicker than in the actual nanowire device. The purpose of specifying this unrealistically large thickness within the SPICE nanowire model was to get the SPICE program to alter the gate capacitance calculations to better reflect those of the experimental devices; by increasing the specified thickness of the gate oxide, the program decreased the gate capacitance. The SPICE code for the device models is displayed in the Appendix. Once device models were constructed, the inverted and buffer sub-circuits were then simulated according to clocking conditions derived from the anticipated millirobot.

IV. Results

A. Logic Analysis and Design for Nanoelectronic Controller

In order to explain the design of the logic control circuit, it is first necessary to discuss the reasoning behind the desired function of the circuit. For any of the legs of the millirobot to move, the electrostatic comb drive motors that provide the mechanical power for each of the legs must resonate at a specific frequency. To achieve resonance, the control circuit must send signals to the electrostatic actuators that oscillate between a high and low voltage. Ideally this would result in a square wave. Because the millirobot designers plan for two electrostatic actuators in a drive train arrangement for each leg system, the control signal to each leg must be composed of two individual square waves that are exactly 90 degrees out of phase, as illustrated in Figure 8. The same such signal can be sent to all three legs in a tripod set, since all three are making the same motion at the same time, as discussed in Section II.A. Further, because each tripod leg set is performing the exact opposite movements at any given time, four signals, two per tripod and the inverses of those two, must be formed by the control circuit. This results in four square waves, each of which is 90 degrees out of phase with two others.

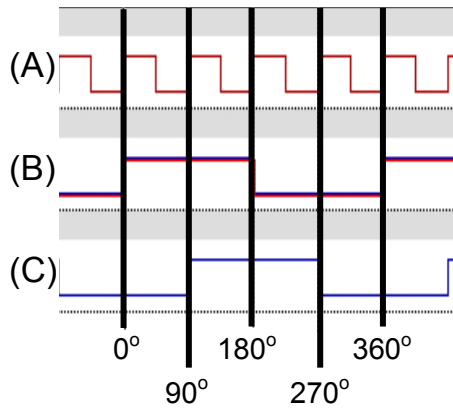


Figure 8. (A) illustrates a seed input signal, (B) is a simulated output signal at 4X the input frequency, (C) is a simulated output signal with a 90° phase shift from (B).

The logic diagram displayed in Figure 6 was designed by the author to form these four square wave signals. As shown in the figure, it is split into four major components, the oscillator, 2-bit counters, tripod switch, and motor driver.

The oscillator component will produce one square wave at a constant frequency, known as the seed signal. This signal will be processed by the rest of the circuit to produce the four output square waves. The oscillator component could be either a conventional microelectronic amplifier circuit or a vibrating crystal. However, both of these types of oscillators are relatively large. New, smaller NEMS (Nano-ElectroMechanical System) oscillators currently under development may provide a much smaller and more viable replacement for these more bulky oscillators [32]. Regardless of the choice of oscillator, the resulting seed signal will be four times the frequency needed to control the comb drive actuators.

The control circuit will produce the two output signals 90 degrees out of phase and at the same frequency, when the seed signal is processed individually by dual 2-bit counters. These two counters are each composed of 2 J-K flip-flops [33-35]. (A J-K flip-flop is described further in Figure 9.) Both 2-bit counters used by this research are very similar in design. The only difference between them is that the first 2-bit counter utilizes the Q output from the initial J-K flip-flop to clock the second J-K flip-flop, while the second counter utilizes the NotQ output from the initial J-K flip-flop to clock the second J-K flip-flop, as highlighted in Figure 6. The design employs this approach in order to hard-wire the second counter to wait one period of the

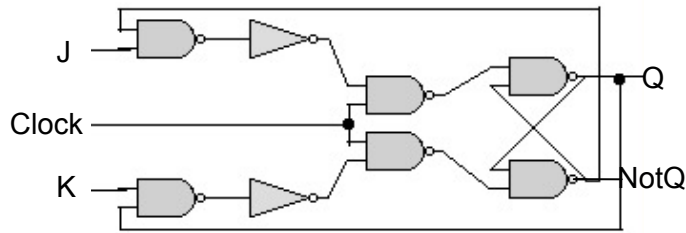


Figure 9. The J-K flip-flop is a conventional logic circuit that utilizes a continuous signal loop to process and then retain multiple values for an indefinite period of time. It will change its stored value to the input line only when the clock is turned on. In essence it is a clocked memory unit.

oscillator before it begins its counting. This delay generates the 90 degree phase shift in the output function of the second counter relative to the output of the first counter.

In order for the control circuit to drive one tripod leg-set forward while the other moves backward, and then reverse the two sets once the legs have reached their full range of motion, the circuit must have a method of detecting when the legs have reached their farthest forward position. Here, this component is termed a “tripod switch”. The tripod switch is composed of two contact switches, one for each leg set, and another J-K flip-flop. The contact switches can have one plate mounted on either the leg, or more easily, on the driving shuttle. In either case, there is a second plate fixed at an appropriate location at the farthest extreme of the leg movement. When the two plates of the switch come in contact, they complete the circuit connecting the J-K flip-flop to a voltage source, creating a value of “1”. The J-K flip-flop changes its stored signal, causing the first tripod set to reverse and the second tripod set to move forward. This separates the two plates of the contact switch and returns the input line to “0”. When the two plates of the second contact switch are touched, a “1” is again pulsed to the J-K flip-flop causing it to change its signal. Through this mechanism, the two contact switches and the motion of the legs become a very low frequency pulse generator.

The output signals from the two counters and the tripod switch are fed into the motor driver, as shown in Figure 6. Here, the signal from the tripod switch is split; one side will remain unaltered while the other side is inverted. The two signals from the tripod switch and the two signals from the counters are combined in a series of four XOR gates, one tripod switch signal with each of the counter signals. The four outputs from the XOR gates will become the outputs

for the entire control circuit. These four signals are all at the correct frequency, and each is 90 degrees out of phase relative to two others. Therefore, the logic is able to control and coordinate the electrostatic actuators that power each of the six legs on a millirobot.

B. Layout of the Nanoelectronic Circuit

The logic circuit described above was successfully mapped to DeHon's nanowire circuit architecture. The final circuit layout is shown in Figure 1. Each of the different cells (grids) corresponds to the block level sections described in Figure 6. The only limitation taken into account during the nanoelectronic circuit design was the limitation due to the effect of undesired fan-out. This effect is caused by voltage leakage through the diode junctions whenever the n-type nanowire is at a high voltage [1]. The effect of undesired fan-out is only a problem when either a prolonged period of high voltage occurs or when there are a large number of diodes connected to one transistor. Due to the small number of diode connections within each circuit element, the effect was not an immediate issue and therefore no circuit redesigns were necessary. However, the possibility of undesired fan-out did prevent the combination of the major block sections (the counters, tripod switch, and motor driver) into one large cell which would have reduced the need for microwire interconnects within the circuit.

C. Nanoelectronic Circuit Simulations

SPICE simulations were run using the nanowire device models shown in the Appendix in order to assess the output signals from the nanoelectronic circuit. The results of these simulations are shown in Figures 10 and 11. The first simulation was of the individual sub-circuits of the inverter and buffer. This simulation produced consistent voltage calculations when compared with results produced by Das et al. who used advanced Cadence simulation software in separate research that also explored some of DeHon's basic circuit designs, though for other purposes [1]. Unexpectedly, the more primitive SPICE simulations used here also have accounted for the effect of undesired fan-out as shown in Figure 10(D) by the decrease in voltage

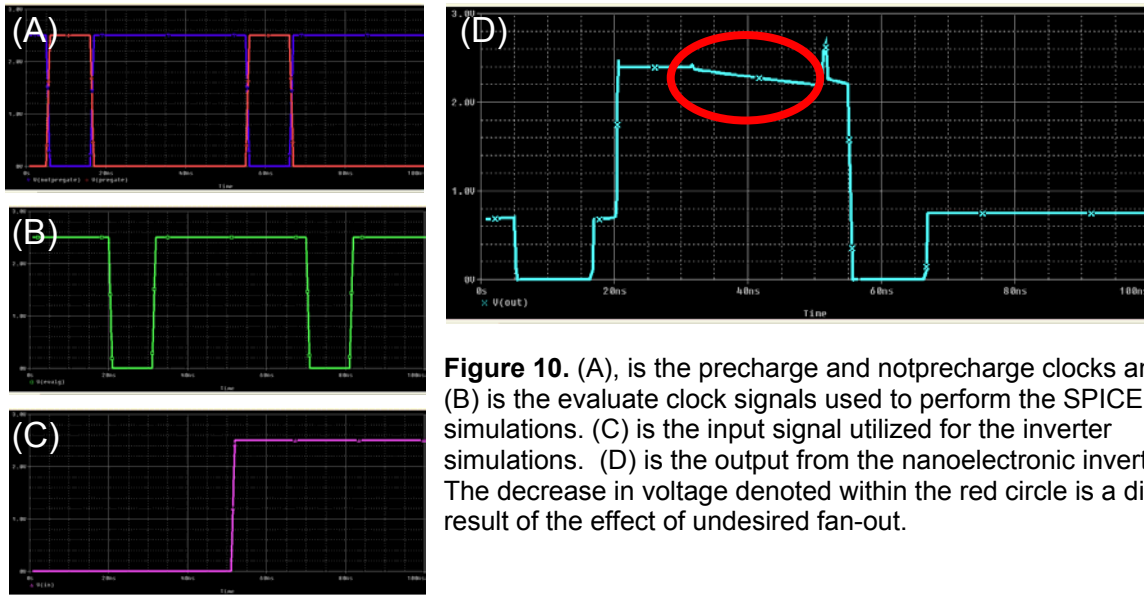
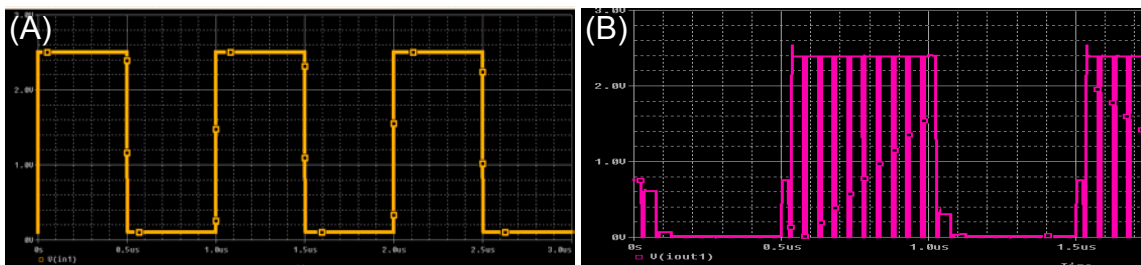


Figure 10. (A), is the precharge and notprecharge clocks and (B) is the evaluate clock signals used to perform the SPICE simulations. (C) is the input signal utilized for the inverter simulations. (D) is the output from the nanoelectronic inverter. The decrease in voltage denoted within the red circle is a direct result of the effect of undesired fan-out.

denoted within the red circle. Unfortunately, these simulations did not accurately project power consumption because of the aforementioned necessarily unrealistic approximations for resistance and capacitance utilized in the SPICE nanowire transistor models.

In order to replicate the manner in which the millirobot control circuit should operate when processing the required signals for the millirobot to function, the second simulation used the predicted oscillator output signal as the input for the full nanowire control circuit. The results from these further simulations, depicted in Figure 11, revealed that the circuit would produce four square waves at four times the frequency of the input and at 90° intervals. While the signal shape was correct, the signal was not as stable as desired at the high voltages need to represent a “1”. As Figure 11(B) illustrates, the output from the simulation oscillates between a

Figure 11. (A) Depicts the optimal output signal from the simulation of the nanoelectronic circuit under relatively high-frequency clocking conditions. (B) Shows the actual, unstable output formed by the nanoelectronic millirobot control circuit.



high and low value when the signal should maintain a constant high voltage. This suggests that the nanoelectronic circuit might not be as reliable as desired for control without a minor adjustment, which is described below.

V. Discussion

Based on the simulation results, the design for the nanoelectronic circuit depicted in Figure 1 is predicted to produce signals of the shape determined by the author to be needed for control of the millirobot. DeHon's nanowire circuit architecture also is predicted to permit the millirobot control circuit to be compact and low-power. In addition, it was found that, because all of the devices in DeHon's architecture "bend" signals at 90° angles (illustrated by the signal paths in Figure 7), looping circuit elements, such as the J-K flip-flop, were easily implemented.

The nanowire SPICE models used in this research accurately represented the voltage characteristics of the nanowire devices. The simulations run using these device models formed square waves at the expected frequencies and spacing. However, the stability of these signals was not immediately sufficient to ensure the reliable control of the comb drive actuators. The uneven depressions in the signal were a direct result of the clocked nature of the circuit, and the necessity to precharge the output by connecting it to the ground as described in the Section II.B.

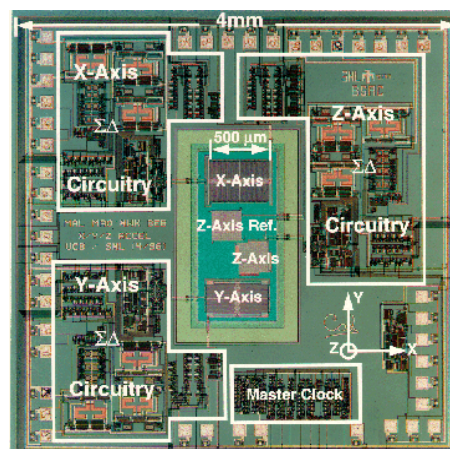
There are several possible solutions for the problem stated above. The primary solution is to include a circuit that acts as a signal filter, removing the drops in voltage from the output signal. Because this filter would have to generate a constant output, it could not be made from the same dynamic architecture that was the cause of the problem. Instead, the filter would be built out of traditional bulk-silicon complementary metal-oxide semiconductor (CMOS) circuitry. There would have to be four copies of this filter circuit, one for each output, each of which would be larger and consume relatively more power than the actual nanowire circuit itself.

VI. Conclusion and Summary

A novel nanoelectronic digital logic circuit was designed to control a millimeter-scale walking robot, using a nanowire-based circuit architecture. This nanoelectronic circuit should be ideal for controlling micromachine systems, such as the millirobot, because of the circuit's extremely small size and relatively low-power consumption. Using a SPICE circuit simulator and unique device models developed in this research, simulations were performed to assess the function and integrity of the nanoelectronic circuit's output. The output signals predicted by these simulations met the requirements of the design, with only a minor signal stability issue. Solutions were proposed to correct this. Thus, it is likely that the nanoelectronic circuit designed here could be useful in addressing the broader issue of further miniaturizing circuit-micromachine systems.

Presently, MEMS are being controlled by CMOS circuits that are approximately ten times larger than the MEMS mechanisms themselves. An example of such a circuit-MEMS system is displayed in Figure 12. Utilizing nanocircuitry such as that developed here, it is hoped that circuit-machine systems might integrate both the control circuit and the MEMS mechanisms in one very small package. These very much smaller, "smart" mechanisms could have many potential applications everywhere MEMS devices presently are being investigated for use: from communication networks, to biomedical therapeutics, to the millirobot addressed in this research.

Figure 12. Typical MEMS acceleration sensor from [36]. This image illustrates that the control circuitry for the MEMS devices is many times larger than the devices themselves. The major goal of this research was to design nanoelectronic circuitry that is on a more appropriate scale, much smaller than present microelectronics, and therefore much more vestal.



Appendix: SPICE Models for Nanowire-Based Devices

```
.model NanowireNFET NMOS(
```

```
* Model is approximation of a nanowire NFET
```

```
* Based on regular MOSFET models
```

```
+Level=3 Tox=300.0E-9 VTO=.7 UO=1350 LAMBDA=0.011 CJ=5e-3 cjsw=1e-11
```

```
.model NanowirePFET PMOS(
```

```
* Model is approximation of a nanowire PFET
```

```
* Based on regular MOSFET models
```

```
+Level=3 Tox=300.0E-9 VTO=-.7 UO=1350 LAMBDA=0.011 CJ=5e-3 cjsw=1e-11
```

Acknowledgements

I would like to thank Dr. James C. Ellenbogen, Principal Scientist of the MITRE Nanosystems Group, for his generous guidance and support over the past two years. I would also like to thank Angelo Piccirillo, Ossining High School Science Research Teacher, for his advice and encouragement. Thanks are extended to several other members of the MITRE Nanosystems Group, especially Dr. Carl Picconatto, Dr. Shamik Das, and Garrett Rose, as well as to Valerie Holmes at Ossining High School.

Bibliography

1. S. Das et al. "Architectures and Simulations for Nanoprocessor Systems Integrated on the Molecular Scale." *Submitted for Publication*.
2. K. S. Kwok, J. C. Ellenbogen: Moletronics: future electronics, *Materials Today*, 28-37 (2002).
3. P. L. Chapman, P. T. Krein: Smaller is Better?, *IEEE Industry Apps. Mag.*, 62-67 (2003).
4. A. K. Ojha: Nano-electronics and nano-computing: status, prospects, and challenges, *Proc. of IEEE Region 5 Conference: Annual Technical and Leadership Workshop*, 85 – 91 (2004).
5. A. DeHon, M. J. Wilson: Nanowire-Based Sublithographic Programmable Logic Arrays. *Proc. of the Intl. Symp. on Field Programmable Gate Arrays* (2004).
6. A. DeHon: Array-Based Architecture for FET-Based, Nanoscale Electronics. *IEEE Transactions on Nanotechnology*, 2, 1, 23-32 (2003).
7. J. R. Heath et al. A Defect-Tolerant Computer Architecture: Opportunities for Nanotechnology, *Science*, 280, 1716-1721 (1998).
8. Y. Huang, X. Duan, Q. Wei, C. M. Lieber: Directed Assembly of One-Dimensional Nanostructures into Functional Networks, *Science*, 291, 630-633 (2001).
9. Y. Cui et al.: High Performance Silicon Nanowire Field Effect Transistors, *Nano Letters*, 3, 2, 149-152 (2003).
10. Y. Cui, C. M. Lieber: Functional Nanoscale Electronic Devices Assembled Using Silicon Nanowire Building Blocks, *Science*, 291, 851-853 (2001).
11. X. Duan, Y. Huang, C. M. Lieber: Nonvolatile Memory and Programmable Logic from Molecule-Gated Nanowires, *Nano Letters*, received February 2002.

12. Simulation Program with Integrated Circuit Emphasis. PSPICE A/D by OrCAD, Cadence Design Systems, Inc., San Jose, California.
13. S. Hollar, A. Flynn, C. Bellew, K. S. J. Pister: Solar Powered 10mg Silicon Robot, *Proc. of 16th Annual Intl. IEEE Conf. on MEMS*, 706-711 (2003).
14. R. Yeh, K. S. J. Pister: Design of Low-Power Silicon Articulated Microrobots, *Berkeley Sensor & Actuator Ctr., Dept. of Electrical Engrg. & Computer Sci., Univ. of Calif., Berkeley*.
15. Y. H. Chee, C. Tsang: Micro-Robot Leg Design for SMART DUST Using Improved Inchworm Motor, *Dept. of Electrical Engrg. & Computer Sci., Univ. of Calif. at Berkeley*.
16. D. L. Odell, J. M. Porter: MicroRobot Conveyance and Propulsion System Using Comb Drive and Parallel Plate Actuators: The ScuttleBot, *Univ. of Calif. Berkeley*.
17. D. Routenberg, J. C. Ellenbogen: Design for a Millimeter-Scale Walking Robot, MP 0W00000010, The MITRE Corporation (2000).
18. R. D. Beer et al. "Biologically Inspired Approaches to Robotics." *Communications of ACM*, 40, 3, 31-38 (1997).
19. B. Lee, I. Lee: The Implementation of the Gaits and Body Structure for Hexapod Robot, *Proc. of the 2001 IEEE Intl. Symp. on Industrial Electronics*, 3, 1959-1964 (2001).
20. E. J. Lerner: Making Micromachines, *American Institute of Physics*, 18-22 (1999).
21. T. Mukherjee, G. K. Fedder: Structured Design of Microelectromechanical Systems, *Dept. of Electrical and Computer Engrg. and The Robotics Institute, Carnegie Mellon Univ.* (1997).
22. C. Livermore et al.: A High-Power MEMS Electric Induction Motor, *Journal of MEMS*, 13, 3, 465-471 (2004).
23. T. Hirano: Design, Fabrication, and Operation of Submicron Gap Comb-Drive Microactuators, *Journal of MEMS*, 1, 1, 52-59 (1992).
24. W. A. Moussa et al.: Investigating the Reliability of Electrostatic Comb Drive Actuators Utilized in Microfluidic and Space Systems Using Finite Element Analysis, 1-12.
25. <http://mems.sandia.gov/scripts/images.asp>
26. D. H. Cobden: Nanowires Begin to Shine, *Nature*, 409, 32-33 (2001).
27. A. B. Greytak et al.: Growth and Transport Properties of Complementary Germanium Nanowire Field-Effect Transistors, *Applied Physics Letters*, 84, 21, 4176-4178 (2004).
28. Y. Cui, X. Duan, J. Hu, C. M. Lieber: Doping and Electrical Transport in Silicon Nanowires, *The Journal of Physical Chemistry*, 104, 22, 5213-5216 (2000).
29. Y. Huang et al.: Logic Gates and Computation from Assembled Nanowire Building Blocks, *Science*, 294, 1313-1317 (2001).
30. M. S. Gudixsen et al: Growth of Nanowire Superlattice Structures for Nanoscale Photonics and Electronics, *Nature*, 415, 617-620 (2002).
31. Available at no cost from:
http://products.engineering.com/community/freeapps/freeapps_mac.htm
32. X. M. H. Huang, C. A. Zorman, M. Mehregany, M. L. Roukes: Quality Factor Issues in Silicon Carbide Nanomechanical Resonators, *The 12th Intl. Conference on Solid State Sensors, Actuators and Microsystems*, Boston, 722-725 (2003).
33. R. C. Jaeger: Microelectronic Circuit Design. McGraw-Hill, 1997.
34. J. M. Rabaey: Digital Integrated Circuits: A Design Perspective *Prentice Hall Electronics and VLSI Series*, Upper Saddle River, New Jersey, 1996.
35. D. V. Bugg: Electronics: Circuits, Amplifiers and Gates, Physics Publishing, The Institute of Physics, London, 1999.
36. <http://www.sandia.gov/mstc/technologies/micromachines/tech-info/overview/>

